Int. J. Electrochem. Sci., 11 **(2016)** 8738 – 8748, doi: 10.20964/2016.10.02

International Journal of
ELECTROCHEMICAL
SCIENCE
www.electrochemsci.org

Short Communication

Antifouling Behavior of a Low-Pressure Cold-Sprayed Cu/Al_2O_3 Composite Coating

Huang Guosheng[*], *Xing Lukuo, Li Xiangbo, Wang Hongren*

Science and Technology on Marine Corrosion and Protection Laboratory, Qingdao, China, 266101,
Luoyang Ship Material Research Institute, Qingdao, China, 266101
[*]E-mail: huanggs@sunrui.net

Received: 15 June 2016 / *Accepted:* 24 July 2016 / *Published:* 6 September 2016

In the present investigation, a Cu/Al_2O_3 composite antifouling coating was designed on Q235 steel to improve the service life of vessels, components and structures used in marine environments. The base Al_2O_3 coat was prepared by flame spraying and the antifouling Cu coat was prepared by cold spraying. The Al_2O_3 layer serves as an insulation layer to separate the copper coating from electrical connection to the steel substrate in case of galvanic corrosion, which also can guarantee the release rate of Cu(I) and Cu(II) ions under cathodic protection conditions. The physical and antifouling performance were examined and the following conclusions were drawn: An excellent Cu/Al_2O_3 antifouling coating can be deposited on the steel substrate. The typical bond strength is about 10MPa between Cu layer and Al_2O_3 layer and bond strength between the Al_2O_3 layer and the substrate was about 20MPa. The antifouling performance, compared to a blank sample (Al_2O_3 coated steel) indicates that the Cu/Al_2O_3 antifouling coating can inhibit 85% of biofouling by barnacles, diatoms and mussels.

Keywords: Oxyacetylene flame spraying, Low pressure cold spray, Antifouling, Corrosion

1. INTRODUCTION

For some special parts of a ship, like the grated inlet of a sea chest, biofouling can block the path of the seawater used for cooling the power system of the ship. Biofouling also can cause the rudder to stick or limit its motion for ship control. The available methods for inhibiting both organic and inorganic growth on wetted substrates are varied but most antifouling systems take the form of protective coatings Chambers et al [1], especially organic coatings. When experiencing high-velocity flow with sand or other hard grained solids, an organic coating will be abraded rapidly. Hence, in these special locations, an organic antifouling coating cannot always provide long lasting protection. Inorganic coatings, especially metallic coatings can provide longer anti-abrasive life than do organic coatings, due to their hardness and high bond strength. Amongst the metals, copper is a relatively environment-friendly antifouling material. The antifouling function of Cu coating is achieved through the release of Cu(I) and Cu(II) to the surrounding water Ding et al [2]. Copper cannot replace steel due to its low structural strength and positive potential. For the same reason, copper coating cannot be deposited directly onto steel substrate due to galvanic corrosion caused by the large potential difference between copper and steel. Additionally, the steel structure is always cathodically protected, which will reduce the corrosion rate of copper, and thus the copper concentration accumulates on the surface.

Ding et al [3] prepared a Cu-Cu_2O coating directly on a steel substrate and investigated its corrosion behavior. The anti-fouling performance was determined directly by the corrosion rate of copper as the effective composites are copper ions. Although the coating had excellent antifouling performance in diatom experiments, in a real situation the coating must be insulated from the underlying steel structure to prevent galvanic corrosion. Furthermore, the steel substrate structures are always cathodic protected, which will also hold back the dissolution rate of the copper, thereby decreasing its anti-fouling capability. To counter this situation, Li et al [4, 5] developed a Cu/Cr_2O_3/Al multilayer coating using plasma spray. A Cr_2O_3 layer served as an insulation layer to separate the copper coating from electrical connection to the steel substrate. In case of galvanic corrosion, an aluminum bond coating serves as a transition layer to eliminate the thermal expansion difference between the Cr_2O_3 and the steel. This coating has excellent anti-abrasive corrosion performance, but the antifouling performance is bad because of penetrating pores that exist in the coating.

To improve the service life, a base Al_2O_3 coat was applied by flame spray, and the antifouling Cu coat was applied by cold spray and flame spray. The Al_2O_3 layer serves as an insulation layer to separate the copper coating from electrical connection to the steel substrate to prevent galvanic corrosion. So doing also assures the release rate of Cu ions under even when the substrate is subjected to cathodic protection.

2. EXPERIMENTAL METHODS

2.1. Structure of Antifouling Coating

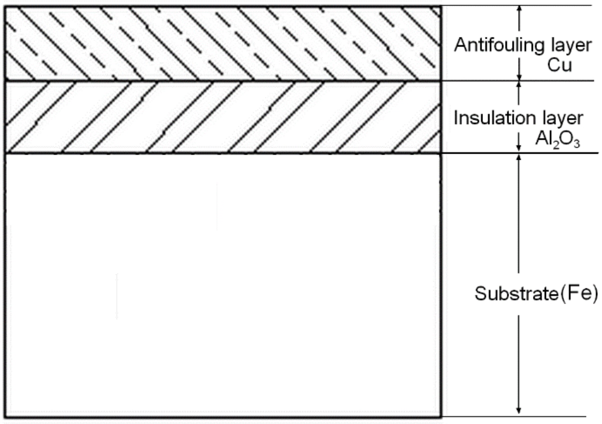

Figure 1. Structure of Cu/Al_2O_3 composite antifouling coating system

A schematic showing the structure of the Cu/Al_2O_3 antifouling coating is shown in Figure 1. For comparison purposes, three kinds of coatings were prepared; these were (1) flame sprayed Al_2O_3 coating, (2) flame sprayed Cu/Al_2O_3 coating and (3) cold sprayed Cu/Al_2O_3 coating.

2.2. Raw Powders

The 99.9% purity commercial copper and alumina powder were provided by Shijiazhuang Gaogong Powder Company. The morphologies of the powders were observed using an SEM (XL-30 Environmental Scanning Electronic Microscope, manufactured by Philips, Netherlands) and is shown in Figure 2. Fused and crushed alumina powder was used for spraying. The powders were mixed on a XSBP 200 screen vibrator (Hangzhou Lantian instrument company, China) for 0.5 hour at a weight ratio 70:30 (copper : alumina). The powder used for flame spraying the Al_2O_3 coating was 100% alumina. The powder used for flame spraying copper coating was 100% copper.

2.3. Flame Spray Cu/Al_2O_3 Coating

The base metal was Q235 steel substrate abraded with emery paper for 15 min. The substrate was preheated to about 90℃ to avoid the effect of moisture and the difference of expansion ratio. A SHF-E2000 oxygen acetylene flame spray system (SULZER company, Switzerland) was adopted for coating application. The oxygen pressure was 0.6 MPa; acetylene pressure was 0.1MPa, and the volume ratio of oxygen to acetylene was l : 1.2 for the preheating gas.

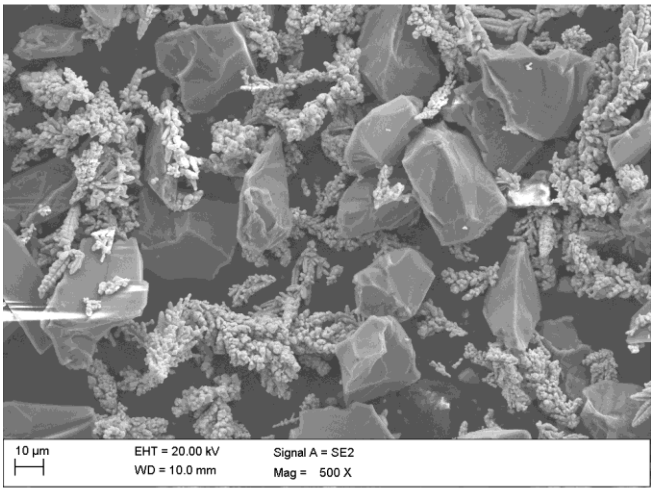

Figure 2. SEM morphology of mixed Cu+Al_2O_3 powders

2.4. Low-Pressure Cold Sprayed Cu/Al_2O_3 Coating

As-sprayed Al_2O_3 coating was used as the substrate. A commercial low-pressure cold spray system, DYMET 413 (Dycomet B. V. Europe, Netherland), was used to deposit the copper coatings.

The nozzle and the gas parameters adopted in this study are listed in Table 1. All samples were prepared using the same parameters. Photograph of cold sprayed Cu/Al_2O_3 coating and thermal sprayed Cu/Al_2O_3 was recorded by Nikon D50 camera (NIKON company, Japan).

Table 1. Summary of nozzle geometric parameters and working conditions of DYMET 413 used for preparing low pressure cold spraying Cu/Al_2O_3 coating on Q235 steel

Parameter	Value
Expansion ratio	3.13
Diameter of nozzle throat	2.54mm
Length of converging part	10mm
Length of diverging part	10mm
Length of elongated part	120mm
Standoff distant from nozzle exit to substrate	20mm
Pressure in prechamber	0. 6MPa
Temperature in prechamber	686K
powder feeding rate	0.51-0.59g/s
Transverse speed of nozzle	20mm/s

2.5. Coating Characterization

The sprayed coatings were cut through their cross-section, abraded with emery paper (grades 280, 600, 1000 and 2000 in sequence), washed with acetone and distilled water, then etched with 10% HCl solution for about 20 seconds. The microstructural characteristics of the etched surfaces were observed using an ULTRA55 scanning electron microscope (SEM, ZEISS Company, German).

The bond strength of all samples were tested on a DWD-20 computer controlled stretcher (CREE instrument company, China) with a 25 mm diameter round sample. The stretching rate is 0.03 mm/s according to standard GB/T 8642-2002.

Resistance of all coating samples between coating and substrate were tested for different area and thickness with an AR907 insulation tester (Shanghai Shuangxu company, China). The voltage between negative probe and positive probe is 200 V.

2.6. Corrosion Behavior

The working electrode for the electrochemical tests was the sprayed coating sample with a size of 10mm × 10mm. A Parr 2273 Potentiostat Electrochemistry Workstation (Ametek Company, America) was used to collect the data. The reference electrode was an SCE; the counter electrode was a Pt electrode, the electrolyte was seawater. The pH was adjusted with KOH to 6.8-7.2. The scan rate for the potential dynamic test was 0.167mV/s. All data were collected after the potential became stable.

2.7. Antifouling Performance

The Antifouling Performance Test for samples conformed strictly to the GB 5370-85 Standard Method for testing antifouling panels in shallow submergence. All samples were immersed vertically in natural seawater at the Maidao test site authenticated by the Chinese Association of Corrosion, which is located in Qingdao. The exposure period was from July to September, which is the most vigorous growth season for macro-organisms in Qingdao. The depth of samples was 1.5m from the sea surface, the temperature varied from 24.5°C to 28.0°C. The amount of sunlight was not controlled.

3. RESULTS AND ANALYSIS

3.1. Characteristics of the Cu/Al_2O_3 Coatings

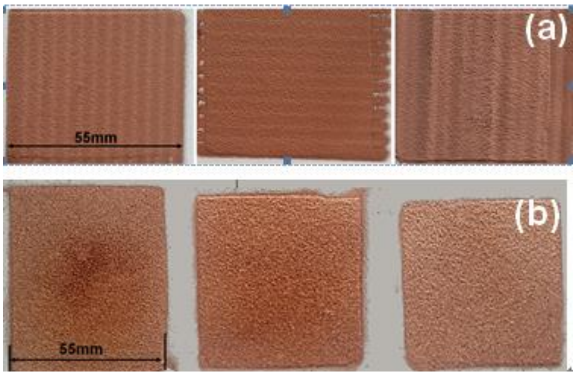

Figure 3. Photograph of Cu/Al_2O_3 coating prepared by (a) low pressure cold spray and (b) flame spray on Q235 Steel

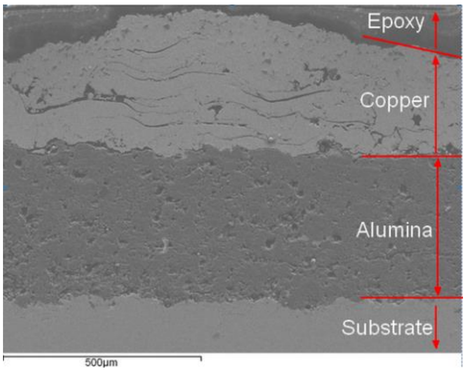

Figure 4. Typical microstructure of low pressure cold sprayed Cu/Al_2O_3 coating (cross-sectional image)

Photographs of the as-sprayed copper coatings are shown in Figure 3. Both flame spray coatings and cold spray coatings had a uniform surface appearance. The surface of the flame sprayed coating was coarser than that of the cold sprayed coating. Many pores could be found on the flame sprayed coating, while the cold sprayed coating appeared to be much dense according to Koivuluoto et. al[6,7]. A typical cross-section of the Cu/Al_2O_3 coating is shown in Figure 4, the bonding between each layer is intimate. The bond strength between each layer is shown in Figure 5. The typical bond strength is about 10MPa between Cu layer and Al_2O_3 layer, bond strength between Al_2O_3 layer and substrate is about 20MPa.

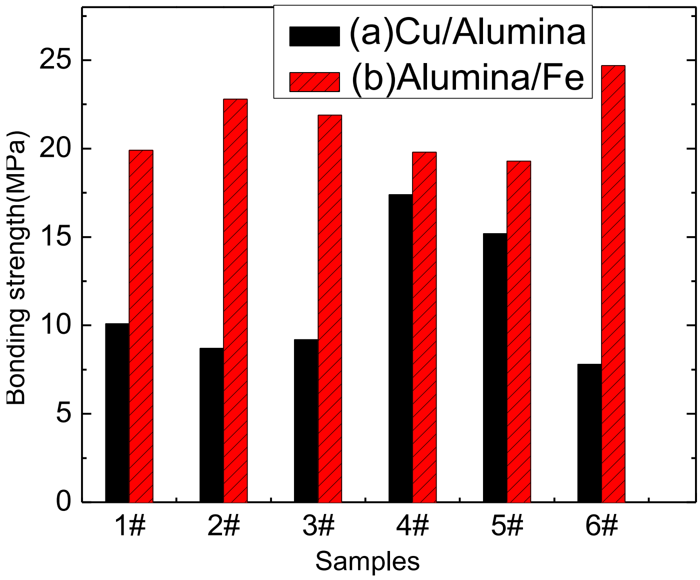

Figure 5. Bond strength between different coating layers, (a) Cu/Al_2O_3 prepared by low pressure cold spraying, (b) Al_2O_3/steel prepared by thermal spraying

3.2. Antifouling Performance

The morphology of all samples after 30 days' immersion is shown in Figure 6. It can be observed that all of the samples failed in the 30 day test according to the criteria of the Standard. The quantity of attached organisms was counted and is documented in Table 2. The organisms occupied an area on the cold sprayed Cu/Al_2O_3 coating of about 14.7% of the flame sprayed Al_2O_3 coating, which meant that the cold sprayed copper coating prevented about 85.3% of the potential biofouling. Comparing to

Table 2. Statistics for attached organisms on panel samples after one month immersion in Maidao test side (1.5m depth and no sunlight controlling)

Type	Average area percentage (%)		
	Barnacles	Diatoms	Mussels
Flame sprayed Al_2O_3 coating	2	87	6
Flame sprayed Cu/Al_2O_3 coating	5	18	37
Cold sprayed Cu/Al_2O_3 coating	3	2	9

It can be seen from Figure 6(b) that corrosion products of iron (red rust labeled with the green arrows) could be found on the surface of the coating.

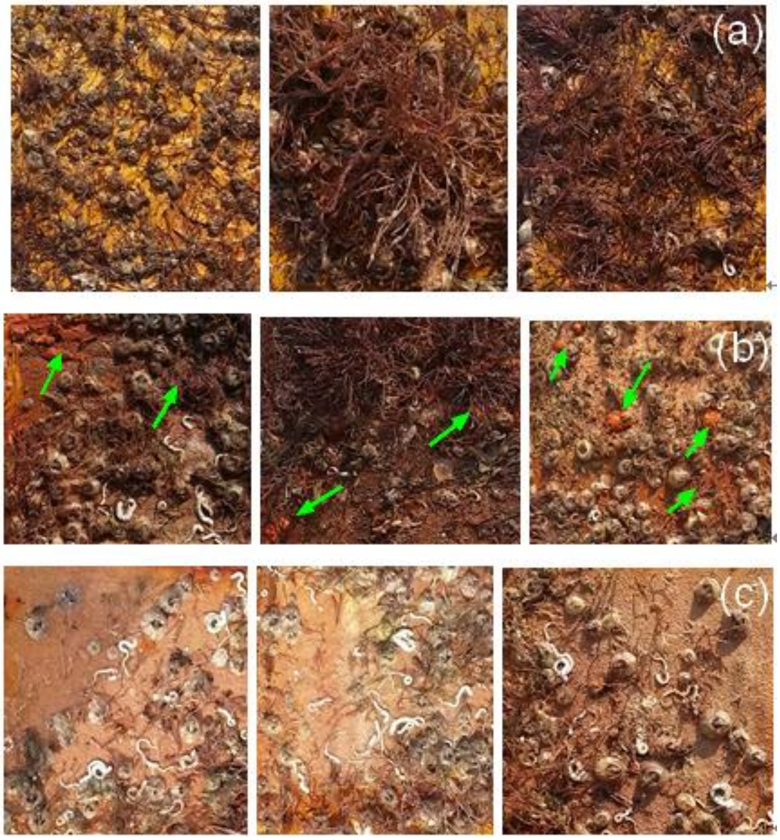

Figure 6. Appearance of biofouling after 30 days immersion, (a) flame sprayed Al_2O_3 coating with epoxy, (b) flame sprayed Cu/Al_2O_3 coating and (c) cold sprayed Cu/Al_2O_3 coating

The resistance of Al_2O_3 between an antifouling layer and the substrate can be seen in Figure 7.

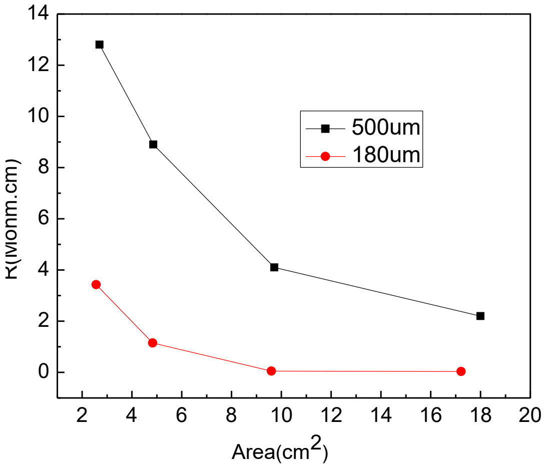

Figure 7. Relationship between coating area and resistance for low pressure cold sprayed Cu/Al_2O_3 coating by

3.3. Corrosion Behavior of Antifouling Coatings

Typical polarization curves for bulk copper, flame sprayed Al_2O_3 coated steel, flame sprayed Cu/Al_2O_3 coated steel and cold sprayed Cu/Al_2O_3 coated steel are shown in Figure 8. It can be seen that all samples has an obviously Tafel region, so the corrosion rate of each samples can be got from Tafel extrapolation methods. The results of polarization curves of coatings in seawater at different immersion times are listed in table 3. The open circuit potential evolution of each samples are also listed in table 3.

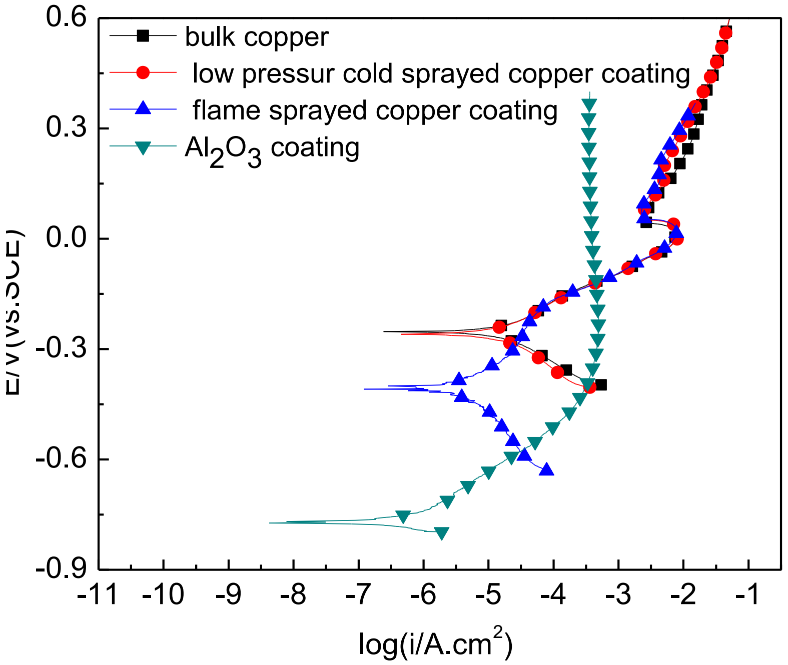

Figure 8. The polarization curves of different samples in natural seawater after 24hrs immersion

Table 3. Variation of open circuit potential and corrosion rate extrapolated from polarization curves for flame sprayed Cu/Al_2O_3 coating and cold sprayed Cu/Al_2O_3 coatings in seawater at different immersion times for 20 d

Immersion time	E(V.SCE)		I_{corr}(μA.cm^{-2})	
	flame sprayed Cu/Al_2O_3	cold sprayed Cu/Al_2O_3	flame sprayed Cu/Al_2O_3	cold sprayed Cu/Al_2O_3
1d	-0.382	-0.212	8.3	15.6
5d	-0.392	-0.231	7.9	12.0
10d	-0.378	-0.199	9.6	12.3
20d	-0.363	-0.221	10.4	12.1

4. DISCUSSION

It can be seen that both thermal spraying and cold spraying can prepare good quality composite Cu/Al_2O_3 coating on steel substrate through the quality analysis. The typical bond strength is about 10MPa between Cu layer and Al_2O_3 layer, bond strength between Al_2O_3 layer and substrate is about 20MPa for cold sprayed coating. According to Li et al [3] the plasma spraying $Cu/Cr_2O_3/Al$ multilayer coating has a porosity about 5%, and the thickness of the coating is limited by the residual stress. While for cold sprayed copper coating , the coating can exceed 300 μm without abscission from Al_2O_3 substrate [8]. That means cold spraying methods can make good physical properties composites coating, the bonding strength and the cross-section verify this point.

It can be seen that the fouling type is different for different samples. In marine environments, the growth activity of each type of organism on a surface is different. Diatoms are most vigorous when no toxicant is present on the surface [9-11], so the larvae of the diatoms will adhere to the surface of samples immersed in seawater. While toxicants are released from the surface, the diatoms will be influenced most, and barnacles will have a higher activity than diatoms. Thus, it can be seen that on nontoxic organic coatings, most biological growth is diatoms. This phenomenon is consistent with Alla [12] experiment if the main fouling organisms are the Barnacles, Diatoms and Mussels.

Although all of the samples failed in the 30 day test according to the criteria of the Standard, the cold sprayed copper coating can prevent about 85.3% biofouling on the substrate. This performance difference is mainly caused by the different releasing rate of copper ion from each coatings. There maybe two reasons that lead to the releasing different, one is the pores type difference, another is the galvanic corrosion existing between coating and substrate. According to Ytreberg [13,14], a lasting releasing rate of about 50μg/cm^2.d can prevent most of the biofouling in stationary seawater. The corresponding releasing rate for cold sprayed Cu/Al_2O_3 is about 110μg/cm^2.d during 20 d immersion, which is far higher than 50μg/cm^2.d. The corresponding releasing rate for flame sprayed Cu/Al_2O_3 is about 80μg/cm^2.d during 20 d immersion, which is far higher than 50μg/cm^2.d. while the antifouling performance of flame sprayed copper coating is much worse than cold sprayed copper coating, which means that's parts of the current density may own to the solving of substrate .

Penetrating pores were present in the flame sprayed Cu/Al_2O_3 coating. Although the alumina coating had a thickness of about 250um and the copper coating had a thickness of about 200um, such coatings cannot avoid the existence of penetrating pores and corrosive media can diffuse to the interface of the substrate down these pores. While for cold sprayed copper coating, the pores inner the coating are all blind. No corrosive media can diffuse to the interface of the substrate down these pores.

The resistance of alumina coating between copper coating and steel substrate determines the corrosion behavior of the coating system. And the resistance can be theoretically calculated using equation (I). In equation (I), R is the resistance, l is the thickness of Al_2O_3 coating, A is the contact area of copper coating and Al_2O_3. ρ is the resistivity of Al_2O_3, and the value is 1015 Ω·cm. For a typical coating system with a thickness of 300 um thickness and an area of 1m^2, the resistance is about 0.01Ω. Actually, the resistance of coating is much higher than calculated value because of the existence of pores and gaps in coating. As in this coating system, the potential difference between copper and steel is approximately 0.3V; this means that the galvanic current would be very high.

However, as in this test experiment, if the coating has no penetrating pores, no corrosion will occur on the steel substrate, whereas for the flame sprayed coating some pores are present in it, and the corrosion of steel will occur. For the cold sprayed coating, all the pores are blind, so no red rust could be found on the surface. For a 500μm thickness coating, a reciprocal relationship was found between the resistance of coating and area of coating. However, for 200μm thick coating, the resistance decreased as the area increased when area was smaller than 10 cm^2. The resistance decreased to 0 as the area exceeded 10 cm^2.

$$R = \rho \frac{l}{A} \qquad \text{(I)}$$

Antifouling performance is determined mainly by the copper ion concentration that accumulates on the surface, and a critical concentration exists for copper to prevent most of the macro-organism growth. The concentration is determined by the corrosion rate of the copper coating in static water. Usually, the copper ion concentration accumulated near the surface under natural conditions varies with the copper type. Pure copper has a high corrosion rate and hence pure copper has few biofouling problems in static marine environments.

The corrosion rate of the metal was obtained by extrapolation of the dynamic polarization curves Ding et al [3]. It can be seen that the corrosion reactions all were determined by anodic active dissolution. For flame sprayed Al_2O_3 coated steel, the corrosion rate was lowest amongst these coatings. The corrosion rate was controlled by the pores in the alumina coating because alumina is inert in seawater. Apparently, the surface was much smaller than for the other samples, on which the metal contacted directly with the water. As the potential shifted more positive, the corrosion current reached a limiting current density and no new reaction occurred. No Cu ions were released from the flame sprayed Al_2O_3 coated steel, so it had the worst antifouling performance. For cold sprayed Cu/ Al_2O_3 coated steel, it had the same corrosion behavior as bulk copper. As the potential shifted to more positive values, the copper experienced the following process: First, anodic active dissolution occurred, which can be written as reaction (1). Second, a new reaction took place, which can be written as reaction (2). It can be inferred that no penetrating pores existed in the cold sprayed coating. In consequence, the cold sprayed copper coating had a similar antifouling performance to pure copper.

The situation was more complicated for flame sprayed Cu/Al_2O_3 coated steel. The corrosion potential was 410mV, about 200mV more negative than copper, but about 350mV more positive compared to steel. That meant the potential was a mixed potential resulting from the copper and the steel [15, 16]. As the corrosion reaction of the steel occurs only through the pores of the coating, so the prevailing reaction is copper dissolution and the potential polarizes more closely towards that of copper. The dissolution rate of copper then decreases because it is cathodically protected by the steel substrate. Correspondingly, the corrosion rate of steel is accelerated. It also can be found that the total current density of thermal sprayed Cu/Al_2O_3 was smaller than that of cold sprayed Cu/Al_2O_3. Hence, it can be inferred that the antifouling performance of cold sprayed Cu/Al_2O_3 will be superior to thermal sprayed Cu/Al_2O_3 coatings.

$$\text{Cu-e} \rightarrow \text{Cu(I)} \qquad (1)$$

$$\text{Cu(I) -e} \rightarrow \text{Cu(II)} \qquad (2)$$

Although above discussion indicates that the antifouling performance of the cold sprayed Cu/ Al_2O_3 coating is superior to former system, it worth noting that antifouling performance is inferior to pure copper. The corrosion rate is closely for copper coating and pure copper, but the surface state is different. The surface of copper coating is much more rough and porous, which will increases the probability of implantation of larvae. And further studied must be down to improve the density and evenness of the cold sprayed copper coating.

5. CONCLUSIONS

The investigation documented above led to the following conclusions:

1) Excellent Cu/Al_2O_3 coatings can be deposited on steel substrates. The typical bond strength between Cu layer and Al_2O_3 layer was about 10MPa, and the bond strength between the Al_2O_3 layer and the substrate was about 20MPa.

2) Antifouling performance tests comparing to a blank sample (an epoxy coated flame sprayed Al_2O_3 coating) indicated that cold sprayed Cu/Al_2O_3 antifouling coatings can inhibit 85.3% of the biofouling activity of barnacles, diatoms and mussels.

References

1. H. Assadi, F. Gärtner, T. Stoltenhoff and H. Kreye, *Acta Materialia*, 51(2003) 4379.
2. L. Chambers, K. Stokes, F. Walsh and R. Wood. *Surf. Coat. Techn.*, 201(2006) 3642.
3. O. Tazegul, V. Dylmishi and H. Cimenoglu, Archives of Civil and Mechanical Engineering, 16(2016) 344.
4. R. Ding, X. Li, J. Wang and L. Xu, *Int. J. Electrochem. Sci.*, 8(2013) 5902.
5. S. Li, L. Xu, C. Shen and L. Xu, *J. Chin. Soc. Corr. Prot.*, 31(2011) 196.
6. H. Koivuluoto, J. Lagerbom, M. Kylmälahti and P. Vuoristo, *J. Therm. Spray Techn.*, 17(2008) 721.
7. N. Kang, P. Coddet, H. Liao and. Christian, *Journal of Alloys and Compounds*. 686(2016) 399.
8. P. Michael, J. Bryan and E. Douglas, *Surface and Coatings Technology*, 297(2016)11.
9. F. Bagley, M. Atlar, A. Charles and C. Anderson, *Ocean Engineering*, 109(2015)595.
10. A. Verween, M. Vincx and S. Degraer, *Biofouling*, 22(2006)221.
11. E. Werner, X. Wang, P. Proksch, C. Perry, R. Osinga, J. Gardères and C. Heinz, Mar. Bio. Techn., 15(2013)375.
12. S. Alla, A. Bazes, J. Mouget and B. Nathalie, *Marine Pollution Bulletin* 64 (2012) 2039.
13. E.Ytreberg, M. Bighiu, L. Lundgren and B. Eklund, *Envir. Poll.*, 213 (2016)594.
14. P. Emilien, B. Claudie, and L. Karine, *Int. J. Mol. Sci.*, 10(2009)3209.
15. D. Rubio, J. Casanueva and E. Nebot, *Applied Therm. Eng.*, (1), 85 (2015) 124.
16. A. Movahedi, J. Zhang, N. Kannc, M. Kasper and N. Magnus, *Progress in Organic Coatings*, 97(2016) 216.